

# DSAC-T: Distributional Soft Actor-Critic with Three Refinements

Jingliang Duan, Wenzuan Wang, Liming Xiao, Jiaxin Gao, and Shengbo Eben Li\*

**Abstract**—Reinforcement learning (RL) has proven to be highly effective in tackling complex decision-making and control tasks. However, prevalent model-free RL methods often face severe performance degradation due to the well-known overestimation issue. In response to this problem, we recently introduced an off-policy RL algorithm, called distributional soft actor-critic (DSAC or DSAC-v1), which can effectively improve the value estimation accuracy by learning a continuous Gaussian value distribution. Nonetheless, standard DSAC has its own shortcomings, including occasionally unstable learning processes and needs for task-specific reward scaling, which may hinder its overall performance and adaptability in some special tasks. This paper further introduces three important refinements to standard DSAC in order to address these shortcomings. These refinements consist of critic gradient adjusting, twin value distribution learning, and variance-based target return clipping. The modified RL algorithm is named as DSAC with three refinements (DSAC-T or DSAC-v2), and its performances are systematically evaluated on a diverse set of benchmark tasks. Without any task-specific hyperparameter tuning, DSAC-T surpasses a lot of mainstream model-free RL algorithms, including SAC, TD3, DDPG, TRPO, and PPO, in all tested environments. Additionally, DSAC-T, unlike its standard version, ensures a highly stable learning process and delivers similar performance across varying reward scales.

**Index Terms**—Reinforcement Learning, Dynamic Programming, Optimal Control, Neural Network

## I. INTRODUCTION

**R**EINFORCEMENT learning (RL) driven by the integration of high-capacity function approximators, such as neural networks, have succeeded in various demanding tasks, ranging from gaming scenarios to robotic control systems [1]–[3]. Despite these achievements, typical model-free RL methods tend to learn unrealistically high state–action values, thereby leading to significant dips in performance. This problem is referred to as value overestimation, which is caused by the maximization operator of Bellman equation applied to noisy value estimates. Such a phenomenon is especially prevalent in deep RL setups due to inaccuracies in value function approximation, as seen in methods like deep Q-network (DQN) [4] and deep deterministic policy gradient (DDPG) [5].

J. Duan and W. Wang contribute equally to this work. All correspondences should be sent to S. Li with email: lisb04@gmail.com.

J. Duan and L. Xiao are with the School of Mechanical Engineering, University of Science and Technology Beijing, China, 100083. Email: duanj1@ustb.edu.cn, xlming@xs.ustb.edu.cn.

W. Wang, J. Gao, and S. E. Li are with the School of Vehicle and Mobility, Tsinghua University, Beijing, China, 100084. Email: wwx.sora@gmail.com, gaojiaxin2017@163.com, lishbo@tsinghua.edu.cn.

Double Q-learning, introduced by Hasselt *et al.* [6], is a pioneering method to mitigate overestimation. It achieves this ability by learning two distinct action value functions, which decouple the maximization operation into action selection and action evaluation. A deep version of this approach, known as double DQN [7], leverages the current Q-network to determine the greedy action, whereas its corresponding target Q-network is utilized to evaluate this action, resulting in a reduced estimation bias in comparison to traditional DQN methods [4]. One shortcoming of these two methods is that they are limited to handling only discrete action spaces. To deal with continuous action spaces, Fujimoto *et al.* [8] proposed clipped double Q-learning, an actor-critic-based approach that incorporates the minimum value between two Q-estimates in formulating the learning objective for both Q-value and policy functions. Since then, this scheme has been widely adopted in mainstream RL algorithms, including twin delayed deep deterministic policy gradient (TD3) [8] and soft actor-critic (SAC) [9], [10], yielding substantial performance enhancements.

The employment of distributional value function is a new designing trend for overestimation mitigation. In [11], we have introduced a standard version of distributional soft actor-critic algorithm (also termed DSAC-v1) to enhance value estimation accuracy by learning a Gaussian distribution of random returns. The standard DSAC aims to learn a distributional value function instead of focusing solely on its expected value (i.e., Q-value). Mathematical analysis has shown that the overestimation bias is inversely proportional to the variance of the value distribution, which builds the theoretical foundation of overestimation mitigation caused by system randomness and approximation errors. Nonetheless, this standard algorithm has a few limitations, notably occasional learning instability and reward scaling sensitivity. The former arises from learning continuous Gaussian value distribution. Unlike conventional RL which focuses solely on expected return [12], standard DSAC incorporates return randomness in the critic gradient, which may easily cause instability in critic updates. The latter emerges from a design dilemma: as standard DSAC uses a fixed boundary to clip target returns, it needs manual adjustments of the reward scale for different tasks to align with the fixed clipping boundary. Consequently, standard DSAC requires task-specific tuning of the reward scale, which limits its adaptability across a range of tasks.

This study proposes an innovative variant of DSAC, which we refer to as DSAC with three refinements (abbreviated as DSAC-T or DSAC-v2). To mitigate occasional learning instability and reward scaling sensitivity, this new algorithm incorporates three important refinements to standard DSAC,

including critic gradient adjusting, twin value distribution learning, and variance-based target return clipping. Our empirical experiments show that DSAC-T outperforms lots of mainstreaming model-free RL algorithms, including SAC, TD3, DDPG, TRPO, and PPO, across all benchmarked tasks. Moreover, compared with standard DSAC [11], DSAC-T exhibits better learning stability and diminishes the necessity for task-specific parameter adjustment. Interested readers can access the source code at <https://github.com/Jingliang-Duan/DSAC-T>. Additionally, DSAC-T is integrated into our self-developed open-source RL toolkit, named GOPS<sup>1</sup> [13]. The key contributions of this paper are as follows:

- 1) We divide the update gradient of value distribution into two parts: (a) mean-related gradient, which incorporates the first-order term of random returns, and (b) variance-related gradient, which includes the second-order term of random returns. While standard DSAC reduces the randomness of variance-related gradient by introducing a target return clipping boundary into gradient calculation, it overlooks the randomness reduction of mean-related gradient. DSAC-T uses an adjusted update gradient to stabilize mean-value updates, where the random target return is replaced with its expected value. This adjustment leads to a similar update rule as non-distributional methods like SAC. Our empirical experiments show that this refinement significantly improves learning stability in practical applications.
- 2) In contrast to standard DSAC, which learns single value distribution, we introduce a distributional version of clipped double Q-learning, called twin value distribution learning. Specifically, DSAC-T trains two independent value distributions and employs the distribution with the lowest Q-value to calculate the gradients for both value distribution and policy function. This approach can further reduce potential overestimation bias, and moreover, it tends to introduce slight underestimation. Underestimation is preferred over overestimation because returns from underestimated actions do not propagate during the critic update.
- 3) During value distribution learning, standard DSAC employs a fixed clipping boundary for target return to prevent gradient explosions, but it is very sensitive to different reward scales. DSAC-T replaces the fixed boundary with a variance-based adjustable value, enabling this algorithm to be more robust to varying reward magnitudes. This modification is straightforward, but highly effective in reducing the necessity for task-specific hyperparameter optimization.

The paper is organized as follows. Section II describes some preliminaries of RL. Section III introduces a distributional soft policy iteration framework for DSAC algorithm design. Section IV proposes DSAC-T by incorporating three new tricks. Section V shows the effectiveness of DSAC-T. Section VII concludes this paper.

<sup>1</sup>Access GOPS at: <https://github.com/Intelligent-Driving-Laboratory/GOPS>

## II. PRELIMINARIES

In this study, we focus on the standard setting of reinforcement learning (RL), where an agent interacts with an environment in discrete time steps. The environment can be represented as a Markov decision process. Both state space  $\mathcal{S}$  and action space  $\mathcal{A}$  are assumed to be continuous. The agent receives feedback from the environment through a bounded reward signal  $r(s_t, a_t)$ . The state transition probability is described as  $p(s_{t+1}|s_t, a_t)$ , mapping a given  $(s_t, a_t)$  to a probability distribution over the next state  $s_{t+1}$ . For simplicity, we denote the current and next state-action pairs as  $(s, a)$  and  $(s', a')$ , respectively. The agent's behavior is defined by a stochastic policy  $\pi(a_t|s_t)$ , which maps a given state to a probability distribution over possible actions. The state and state-action distributions induced by  $\pi$  are denoted as  $\rho_\pi(s)$  and  $\rho_\pi(s, a)$ , respectively.

### A. Maximum Entropy RL

The aim of conventional RL is to find a policy that optimizes the expected accumulated return. In this study, we consider an entropy-augmented objective function [14], which supplements the reward signal with policy entropy:

$$J_\pi = \mathbb{E}_{(s_i \geq t, a_i \geq t) \sim \rho_\pi} \left[ \sum_{i=t}^{\infty} \gamma^{i-t} [r_i + \alpha \mathcal{H}(\pi(\cdot|s_i))] \right], \quad (1)$$

where  $\gamma \in (0, 1)$  is the discount factor,  $\alpha$  is the temperature coefficient, and the policy entropy  $\mathcal{H}$  is expressed as

$$\mathcal{H}(\pi(\cdot|s)) = \mathbb{E}_{a \sim \pi(\cdot|s)} [-\log \pi(a|s)].$$

We denote the entropy-augmented accumulated return from  $s_t$  as  $G_t = \sum_{i=t}^{\infty} \gamma^{i-t} [r_i - \alpha \log \pi(a_i|s_i)]$ , also referred to as soft return. The soft Q-value of  $\pi$  is given as

$$Q^\pi(s_t, a_t) = r_t + \gamma \mathbb{E}_{(s_{i>t}, a_{i>t}) \sim \rho_\pi} [G_{t+1}], \quad (2)$$

which delineates the expected soft return for choosing  $a_t$  in state  $s_t$  and subsequently following policy  $\pi$ .

The ideal policy can be found through a maximum entropy variant of policy iteration. This framework consists of two alternating stages: (a) soft policy evaluation and (b) soft policy improvement, collectively known as soft policy iteration. Provided a policy  $\pi$ , we can continually apply the self-consistency operator  $\mathcal{T}^\pi$  under policy  $\pi$  to learn the soft Q-value, which is depicted as follows:

$$\mathcal{T}^\pi Q^\pi(s, a) = r + \gamma \mathbb{E}_{s' \sim p, a' \sim \pi} [Q^\pi(s', a') - \alpha \log \pi(a'|s')]. \quad (3)$$

On the other hand, the objective of soft policy improvement is to identify a new policy  $\pi_{\text{new}}$  that surpasses the current policy  $\pi_{\text{old}}$ , such that  $J_{\pi_{\text{new}}} \geq J_{\pi_{\text{old}}}$ . Therefore, the policy can be updated directly by maximizing the entropy-augmented objective (1), which is equivalent to

$$\pi_{\text{new}} = \arg \max_{\pi} \mathbb{E}_{s \sim \rho_\pi, a \sim \pi} [Q^{\pi_{\text{old}}}(s, a) - \alpha \log \pi(a|s)]. \quad (4)$$

Any soft policy iteration algorithms that alternate between (3) and (4) can gradually converge to the optimal maximum entropy policy. This property has been mathematically proved in [14] and [9].

### III. DISTRIBUTIONAL SOFT ACTOR-CRITIC

This section begins by introducing the distributional soft policy iteration (DSPI) framework, which was derived in our previous work [11]. This framework extends maximum entropy RL into a distributional learning version. Subsequently, we outline the standard DSAC algorithm (i.e., DSAC-v1) that roots in this framework.

#### A. Distributional Soft Policy Iteration

Let us first define a random variable called soft state-action return:

$$Z^\pi(s_t, a_t) := r_t + \gamma G_{t+1},$$

which is a function of policy  $\pi$  and state-action pair  $(s_t, a_t)$ . The randomness of this variable is attributed to state transition and policy. From (2), we can observe that

$$Q^\pi(s, a) = \mathbb{E}[Z^\pi(s, a)]. \quad (5)$$

One needs to model the distribution of random variable  $Z^\pi(s, a)$ . We define the function  $\mathcal{Z}^\pi(Z^\pi(s, a)|s, a)$  as a mapping from  $(s, a)$  to a distribution over the soft state-action return  $Z^\pi(s, a)$ . This mapping is referred to as soft state-action return distribution or simply value distribution. Relying on this definition, the distributional version of the self-consistency operator in (3) becomes

$$\mathcal{T}_D^\pi Z(s, a) \stackrel{D}{=} r + \gamma(Z(s', a') - \alpha \log \pi(a'|s')), \quad (6)$$

where  $s' \sim p$ ,  $a' \sim \pi$ , and  $A \stackrel{D}{=} B$  indicates that two random variables,  $A$  and  $B$ , have identical probability laws.

We have proved that DSPI, which alternates between (4) and (6), converges uniformly to the optimal policy. Details can be found in [11, Appendix A]. Equation (6) defines a new random variable  $\mathcal{T}_D^\pi Z(s, a)$ , and its distribution is denoted as  $\mathcal{T}_D^\pi \mathcal{Z}(\cdot|s, a)$ . To solve (6), we can update the value distribution by

$$\mathcal{Z}_{\text{new}} = \arg \min_{\mathcal{Z}} \mathbb{E}_{(s, a) \sim \rho_\pi} [D_{\text{KL}}(\mathcal{T}_D^\pi \mathcal{Z}_{\text{old}}(\cdot|s, a), \mathcal{Z}(\cdot|s, a))], \quad (7)$$

where  $D_{\text{KL}}$  is the Kullback-Leibler (KL) divergence. Note that  $D_{\text{KL}}$  can be replaced by other distance measures of two distributions. In fact, DSPI serves as the basic framework for developing distributional soft actor-critic algorithms, including DSAC-v1 in [11] and DSAC-T in this paper.

#### B. Standard DSAC Algorithm

To handle continuous state and action spaces, our previous study has proposed a standard version of DSAC algorithm (DSAC-v1), which employs neural networks as the approximators of both value function and policy function [11]. The value distribution and stochastic policy are parameterized as  $\mathcal{Z}_\theta(\cdot|s, a)$  and  $\pi_\phi(\cdot|s)$ , where  $\theta$  and  $\phi$  are network parameters. Here, we model these two parameterized functions as diagonal Gaussian, with mean and standard deviation as their outputs. Similar to most RL methods, this algorithm follows a cycle of policy evaluation (critic update) and policy improvement (actor update).

1) *Policy Evaluation:* According to (7), the critic is updated by minimizing

$$J_{\mathcal{Z}}(\theta) = \mathbb{E}_{(s, a) \sim \mathcal{B}} [D_{\text{KL}}(\mathcal{T}_D^{\pi_{\bar{\phi}}} \mathcal{Z}_{\bar{\theta}}(\cdot|s, a), \mathcal{Z}_\theta(\cdot|s, a))], \quad (8)$$

where  $\mathcal{B}$  denotes the replay buffer of historical samples, while  $\bar{\theta}$  and  $\bar{\phi}$  are the parameters of target networks. Given that  $\mathcal{T}_D^{\pi_{\bar{\phi}}} \mathcal{Z}_{\bar{\theta}}(\cdot|s, a)$  is unknown, we develop a sample-based version of (8):

$$J_{\mathcal{Z}}(\theta) = - \mathbb{E}_{\substack{(s, a, r, s') \sim \mathcal{B}, a' \sim \pi_{\bar{\phi}}, \\ Z(s', a') \sim \mathcal{Z}_{\bar{\theta}}(\cdot|s', a')}} [\log \mathcal{P}(y_z | \mathcal{Z}_\theta(\cdot|s, a))], \quad (9)$$

where  $y_z$  is the target value for random return:

$$y_z = r + \gamma(Z(s', a') - \alpha \log \pi_{\bar{\phi}}(a'|s')). \quad (10)$$

For simplicity of exposition, the subscript  $(s, a, r, s') \sim \mathcal{B}$ ,  $a' \sim \pi_{\bar{\phi}}$ ,  $Z(s', a') \sim \mathcal{Z}_{\bar{\theta}}(\cdot|s', a')$  of  $\mathbb{E}$  will be dropped if it can be inferred from the context. Given that  $\mathcal{Z}_\theta$  is assumed to be Gaussian, it can be expressed as  $\mathcal{Z}_\theta(\cdot|s, a) = \mathcal{N}(Q_\theta(s, a), \sigma_\theta(s, a)^2)$ , where  $Q_\theta(s, a)$  and  $\sigma_\theta(s, a)$  are the mean and standard deviation of value distribution. Combining this with (9), the critic update gradient is

$$\begin{aligned} \nabla_\theta J_{\mathcal{Z}}(\theta) &= \mathbb{E} \left[ \nabla_\theta \frac{(y_z - Q_\theta(s, a))^2}{2\sigma_\theta(s, a)^2} + \frac{\nabla_\theta \sigma_\theta(s, a)}{\sigma_\theta(s, a)} \right] \\ &= \mathbb{E} \left[ \underbrace{-\frac{(y_z - Q_\theta(s, a))}{\sigma_\theta(s, a)^2} \nabla_\theta Q_\theta(s, a)}_{\text{mean-related gradient}} \right. \\ &\quad \left. - \underbrace{\left( \frac{(y_z - Q_\theta(s, a))^2}{\sigma_\theta(s, a)^3} - \frac{1}{\sigma_\theta(s, a)} \right) \nabla_\theta \sigma_\theta(s, a)}_{\text{variance-related gradient}} \right]. \end{aligned} \quad (11)$$

The critic gradient consists of two components: mean-related gradient and variance-related gradient. The difference between  $y_z$  and  $Q_\theta(s, a)$  can be viewed as a random version of temporal difference (TD) error. The presence of squared TD error in the variance-related gradient makes the critic gradient  $\nabla_\theta J_{\mathcal{Z}}(\theta)$  susceptible to explode as  $|\text{TD}| \rightarrow \infty$ , which may lead to learning instability. To mitigate this issue, we use a technique that clips  $y_z$  in the variance-related gradient term, ensuring it stays in proximity to the mean value of the current value distribution. This technique lends stability to the learning progression of standard deviation  $\sigma_\theta(s, a)$ . The clipping function is defined as

$$C(y_z) := \text{clip}(y_z, Q_\theta(s, a) - b, Q_\theta(s, a) + b), \quad (12)$$

where  $b$  is the clipping boundary. After clipping, the critic gradient (11) becomes

$$\begin{aligned} \nabla_\theta J_{\mathcal{Z}}(\theta) &\approx \mathbb{E} \left[ -\frac{(y_z - Q_\theta(s, a))}{\sigma_\theta(s, a)^2} \nabla_\theta Q_\theta(s, a) \right. \\ &\quad \left. - \left( \frac{(C(y_z) - Q_\theta(s, a))^2}{\sigma_\theta(s, a)^3} - \frac{1}{\sigma_\theta(s, a)} \right) \nabla_\theta \sigma_\theta(s, a) \right]. \end{aligned} \quad (13)$$

Moreover, the target networks employ a slow-moving update mechanism to ensure a relatively stable target distribution for critic updating.

2) *Policy Improvement*: The actor is improved by maximizing a parameterized version of (4):

$$\begin{aligned} J_\pi(\phi) &= \mathbb{E}_{s \sim \mathcal{B}, a \sim \pi_\phi} \left[ \mathbb{E}_{Z(s, a) \sim \mathcal{Z}_\theta(\cdot | s, a)} [Z(s, a)] - \alpha \log(\pi_\phi(a | s)) \right] \\ &= \mathbb{E}_{s \sim \mathcal{B}, a \sim \pi_\phi} [Q_\theta(s, a) - \alpha \log(\pi_\phi(a | s))], \end{aligned} \quad (14)$$

whose gradient can be trivially estimated using the reparameterization trick [11]. In contrast to Q-values, the value distribution offers a richer set of predictions for policy learning. As an illustration, one can choose to incorporate the variance of the value distribution into objective (14) to promote risk-sensitive policy learning [15].

The temperature parameter  $\alpha$  plays an important role in balancing exploitation and exploration. Following similar idea in [10], we update this parameter using

$$\alpha \leftarrow \alpha - \beta_\alpha \mathbb{E}_{s \sim \mathcal{B}, a \sim \pi_\phi} [-\log \pi_\phi(a | s) - \bar{\mathcal{H}}], \quad (15)$$

where  $\bar{\mathcal{H}}$  stands for the target entropy and  $\beta_\alpha$  is the learning rate. Drawing from the discussion above, standard DSAC can be implemented by iterative updating the value distribution, policy, and temperature parameter through stochastic gradient descent (refer to [11] for more details).

#### IV. DSAC WITH THREE REFINEMENTS (DSAC-T)

The previous section introduces a standard DSAC algorithm that incorporates a distributional value function rather than an expected value function in critic and actor updates. This algorithm is practically useful, but occasionally leads to unstable learning processes in some tasks. Moreover, it requires task-specific hyperparameter tuning, which is inconvenient in fast task setups. In this section, we add three important refinements to standard DSAC, aiming to bolster learning stability and diminish sensitivity to reward scaling. These three refinements include critic gradient adjusting, twin value distribution learning, and variance-based target return clipping. As a result, we develop an enhanced version of DSAC, named DSAC with three refinements (DSAC-T) or, alternatively, DSAC-v2.

##### A. Critic gradient adjusting

As delineated in (13), DSAC-v1 reduces the randomness in variance-related gradient through clipping the random target return. Nonetheless, this method cannot address the high randomness in mean-related gradient prompted by the random target return. To rectify this issue, our basic idea is to adjust the mean-related gradient by replacing the random target return with a steadier surrogate function.

We initially turn our attention to the target value used for Q-network updates in non-distributional methods:

$$y_q = r + \gamma(Q_{\bar{\theta}}(s', a') - \alpha \log \pi_{\bar{\theta}}(a' | s')), \quad (16)$$

where  $a' \sim \pi_{\bar{\theta}}(\cdot | s')$ . Compared with target Q-value  $y_q$  in (16), the target return  $y_z$  in (10) contains more randomness due to the value distribution  $\mathcal{Z}$ . As indicated by the critic update gradient in (13), this can lead to instability during the learning of value distribution.

From (5), we can show the equivalence between  $y_z$  and  $y_q$ :

$$\begin{aligned} &\mathbb{E}_{Z(s', a') \sim \mathcal{Z}_{\bar{\theta}}(s', a')} \left[ y_z \Big|_{a' \sim \pi_{\bar{\theta}}, Z(s', a') \sim \mathcal{Z}_{\bar{\theta}}(\cdot | s', a')} \right] \\ &= r + \gamma(Q_{\bar{\theta}}(s', a') - \alpha \log \pi_{\bar{\theta}}(a' | s')) \Big|_{a' \sim \pi_{\bar{\theta}}} \\ &= y_q. \end{aligned} \quad (17)$$

Leveraging this equivalence, we can substitute the first occurrence of  $y_z$  in (13) with  $y_q$ . Then, we rewrite (13) as a adjusted version:

$$\begin{aligned} \nabla_\theta J_{\mathcal{Z}}(\theta) &\approx \mathbb{E} \left[ -\frac{(y_q - Q_\theta(s, a))}{\sigma_\theta(s, a)^2} \nabla_\theta Q_\theta(s, a) \right. \\ &\quad \left. - \left( \frac{(C(y_z) - Q_\theta(s, a))^2}{\sigma_\theta(s, a)^3} - \frac{1}{\sigma_\theta(s, a)} \right) \nabla_\theta \sigma_\theta(s, a) \right]. \end{aligned} \quad (18)$$

Since  $y_q$  is more certain than  $y_z$ , this adjusted critic gradient can reduce the high randomness in mean-related gradient. Note that  $y_q - Q_\theta(s, a)$  precisely represents the TD error. Consequently, the first term in (18) is equivalent to the update gradient of Q-value in non-distributional RL methods, but scaled by an adjustment factor  $\sigma_\theta(s, a)^2$ . By viewing  $Q_\theta(s, a)$  and  $\sigma_\theta(s, a)$  as independent entities, the new Q-value learning mechanism delineated by (18) parallels existing RL methods like soft actor-critic (SAC) [9], which ensures comparable learning stability.

##### B. Twin value distribution learning

The second refinement is a distributional variation of clipped double Q-learning [8], called twin value distribution learning. Specifically, we parameterize two value distributions, characterized by parameters  $\theta_1$  and  $\theta_2$ , which are trained independently. The value distribution with the smaller mean value is chosen to construct critic and actor gradients. For critic updating, we define the index of the chosen value distribution as

$$\bar{i} := \arg \min_{i=1,2} Q_{\bar{\theta}_i}(s', a') \Big|_{a' \sim \pi_{\bar{\theta}}(\cdot | s')}. \quad (19)$$

Subsequently, we use  $\bar{\theta}_{\bar{i}}$  to evaluate the target return in (10) and the target Q-value in (16). The expressions for these target evaluations are shown as follows:

$$\begin{aligned} y_z^{\min} &= r + \gamma(Z(s', a') - \alpha \log \pi_{\bar{\theta}}(a' | s')) \Big|_{Z(s', a') \sim \mathcal{Z}_{\bar{\theta}_{\bar{i}}}(\cdot | s', a')}, \\ y_q^{\min} &= r + \gamma(Q_{\bar{\theta}_{\bar{i}}}(s', a') - \alpha \log \pi_{\bar{\theta}}(a' | s')). \end{aligned} \quad (20)$$

By inserting (20) into (18), it follows that

$$\begin{aligned} \nabla_{\theta_i} J_{\mathcal{Z}}(\theta_i) &\approx \mathbb{E} \left[ -\frac{(y_q^{\min} - Q_{\theta_i}(s, a))}{\sigma_{\theta_i}(s, a)^2} \nabla_{\theta_i} Q_{\theta_i}(s, a) \right. \\ &\quad \left. - \left( \frac{(C(y_z^{\min}) - Q_{\theta_i}(s, a))^2}{\sigma_{\theta_i}(s, a)^3} - \frac{1}{\sigma_{\theta_i}(s, a)} \right) \nabla_{\theta_i} \sigma_{\theta_i}(s, a) \right]. \end{aligned} \quad (21)$$

In a similar manner, the actor objective undergoes a revision of twin value distributions:

$$J_\pi(\phi) = \mathbb{E}_{s \sim \mathcal{B}, a \sim \pi_\phi} [\min_{i=1,2} Q_{\theta_i}(s, a) - \alpha \log(\pi_\phi(a | s))]. \quad (22)$$

In contrast to the single value distribution used in DSAC-1, DSAC-T employs the minimization of twin value distributions

to shape the target distribution in the critic update. This approach is able to further mitigate overestimation bias, and moreover, it has the tendency to yield slight underestimation. It is important to highlight that minor underestimation is generally more desirable than overestimation. This is because overestimated action values can propagate during learning, whereas underestimated actions typically get sidestepped by the policy, preventing their values from propagating. Additionally, the underestimation of Q-values can serve as a performance lower bound for policy optimization, which is helpful to improve learning stability.

### C. Variance-based target return clipping

As per (12), DSAC-v1 adopts a fixed clipping boundary to prevent gradient explosions. The choice of this clipping boundary is of significant importance, as a smaller value can impact the accuracy of variance learning, while a larger value may lead to a huge gradient norm. An improper selection of clipping boundaries may severely hinder learning performance. It is important to recognize that the mean and variance of value distribution have a direct relationship with reward magnitudes. This indicates that different reward scales typically correspond to distinct optimal clipping boundary designs. Moreover, reward magnitudes can vary not only across diverse tasks but also evolve over time as the policy improves during training. Therefore, DSAC-v1 often needs manual adjustment of reward scales for each specific task, which is a non-trivial job in itself.

To alleviate this sensitivity to reward scaling, our refined version automates the clipping boundary determination by

$$b = \xi \mathbb{E}_{(s,a) \sim \mathcal{B}} [\sigma_{\theta_i}(s, a)], \quad (23)$$

where  $\xi$  is a constant parameter that controls the clipping range. In this setup, the boundary can adapt to varying reward magnitudes across varied tasks and training phases. Compared to the direct adjustment of  $b$ , selecting  $\xi$  is more straightforward, as (23) inherently correlates with reward magnitude. Typically, we can set  $\xi = 3$  following the three-sigma rule. While this refinement is straightforward, it is remarkably effective, eliminating the necessity for task-specific hyperparameter fine-tuning. Finally, DSAC-T is detailed in Algorithm 1.

## V. EXPERIMENTAL VALIDATION

We assess the performance of DSAC-T by conducting a series of continuous control tasks in MuJoCo [16]. These tasks are facilitated through the OpenAI Gym interface. The benchmark tasks utilized in this study are depicted in Fig. 1, including Humanoid, Ant, HalfCheetah, InvertedDoublePendulum, and Walker2d. All baseline algorithms used are accessible in GOPS [13], an open-source RL solver developed with PyTorch.

### A. Baselines

Our algorithm is evaluated against well-known model-free algorithms. These include deep deterministic policy gradient (DDPG) [5], trust region policy optimization (TRPO) [17], proximal policy optimization (PPO) [18], twin delayed deep

---

### Algorithm 1 DSAC-T

---

```

Input:  $\theta_1, \theta_2, \phi, \alpha, \beta_Z, \beta_\pi, \beta_\alpha, \tau$ 
Initialize target networks:  $\bar{\theta}_1 \leftarrow \theta_1, \bar{\theta}_2 \leftarrow \theta_2, \bar{\phi} \leftarrow \phi$ 
for each iteration do
  for each sampling step do
    Calculate action  $a \sim \pi_\phi(a|s)$ 
    Get reward  $r$  and new state  $s'$ 
    Store samples  $(s, a, r, s')$  in buffer  $\mathcal{B}$ 
  end for
  for each update step do
    Sample data from  $\mathcal{B}$ 
    Update critic using  $\theta \leftarrow \theta - \beta_Z \nabla_\theta J_Z(\theta)$ 
    Update actor using  $\phi \leftarrow \phi + \beta_\pi \nabla_\phi J_\pi(\phi)$ 
    Update temperature using (15)
    Update target networks using
       $\bar{\theta} \leftarrow \tau\theta + (1 - \tau)\bar{\theta}, \bar{\phi} \leftarrow \tau\phi + (1 - \tau)\bar{\phi}$ 
  end for
end for

```

---

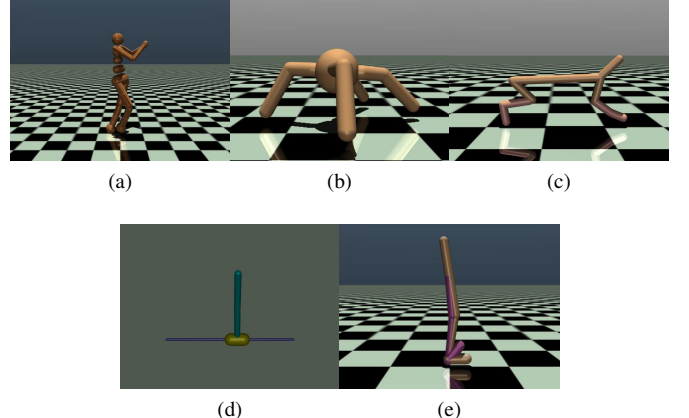


Fig. 1. Benchmarks. (a) Humanoid-v3:  $(s \times a) \in \mathbb{R}^{376} \times \mathbb{R}^{17}$ . (b) Ant-v3:  $(s \times a) \in \mathbb{R}^{111} \times \mathbb{R}^8$ . (c) HalfCheetah-v3:  $(s \times a) \in \mathbb{R}^{17} \times \mathbb{R}^6$ . (d) InvertedDoublePendulum-v3:  $(s \times a) \in \mathbb{R}^6 \times \mathbb{R}^1$ . (e) Walker2d-v3:  $(s \times a) \in \mathbb{R}^{17} \times \mathbb{R}^6$ .

deterministic policy gradient (TD3) [8], and soft actor-critic (SAC) [10]. These baselines have been widely tested and employed across a range of demanding domains. By comparing with these algorithms, we aim to provide an objective evaluation of DSAC-T. To assess the effectiveness of the refinements about learning stability, we also draw comparisons between DSAC-T and DSAC-v1. Both versions employ an adaptive clipping boundary as detailed in (23), with  $\xi = 3$ .

To maintain fairness in comparison, our DSAC-T algorithm is also implemented in GOPS, ensuring an identical modular architecture. Both actor and critic are built with a multi-layer perceptron comprising three hidden layers, each with 256 units and GELU. For the value distribution and stochastic policy, we employ a diagonal Gaussian distribution. Specifically, each neural network projects the input states to the mean and standard deviation. The Adam optimization method is employed for all parameter updates. All algorithms, including baselines and DSAC-T, follow a similar network architecture and use equivalent hyperparameters. More detailed hyperparameters

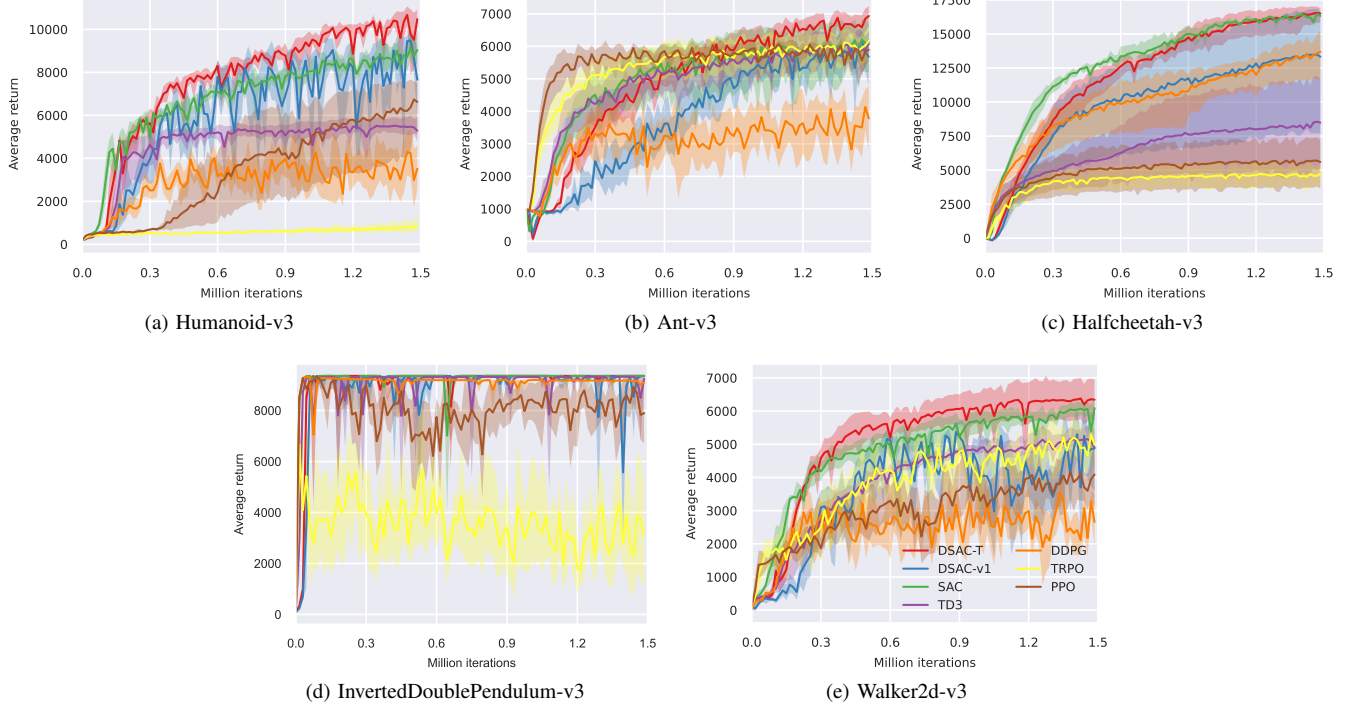


Fig. 2. Training curves on benchmarks. The solid lines correspond to mean and shaded regions correspond to 95% confidence interval over 5 runs. The iteration of PPO and TRPO is counted by the number of network updates.

are provided in Table I.

TABLE I  
DETAILED HYPERPARAMETERS.

Hyperparameters	Value
<i>Shared</i>	
Optimizer	Adam ( $\beta_1 = 0.9, \beta_2 = 0.999$ )
Actor learning rate	1e-4
Critic learning rate	1e-4
Discount factor ( $\gamma$ )	0.99
Policy update interval	2
Target smoothing coefficient ( $\tau$ )	0.005
Reward scale	1
<i>Maximum-entropy framework</i>	
Learning rate of $\alpha$	3e-4
Expected entropy ( $\bar{\mathcal{H}}$ )	$\bar{\mathcal{H}} = -\dim(\mathcal{A})$
<i>Deterministic policy</i>	
Exploration noise	$\epsilon \sim \mathcal{N}(0, 0.1^2)$
<i>Off-policy</i>	
Replay buffer size	$1 \times 10^6$
Sample batch size	20
<i>On-policy</i>	
Sample batch size	2000
Replay batch size	2000

## B. Results

We conducted five separate tests for each algorithm, using distinct but consistent random seeds across all algorithms. Learning curves and policy performance are presented in Fig. 2 and Table II, respectively. Our results reveal that DSAC-T surpasses (at least matches) the performance of all baseline algorithms across all benchmark tasks. Taking Humanoid-v3 as an example, compared with SAC, TD3, PPO, DDPG, and

TRPO, our algorithm shows relative improvements of 17.2%, 94.2%, 59.2%, 106.7%, and 1032.9%, respectively. These results suggest that DSAC-T sets a new standard of performance for model-free RL algorithms. Moreover, compared to its predecessor (DSAC-v1), this new version (DSAC-T) has achieved substantial enhancements in both learning stability and final outcomes.

Table III showcases the relative estimation bias for each algorithm. While both DSAC-v1 and DDPG utilize a single critic (excluding the target critic) in an off-policy manner, DSAC-v1 exhibits lower overestimation bias overall. This suggests that value distribution learning can partly counteract overestimation issues. By incorporating the twin value distribution learning technique, DSAC-T further reduces overestimation bias, leading to a minor underestimation in certain benchmarks. As a result, DSAC-T achieves enhanced learning stability compared to DSAC-v1. Guided by the principle that underestimation is preferred over overestimation when biases are of similar magnitude, the estimation accuracy of DSAC-T either surpasses or at least aligns with all baselines across various benchmarks.

## C. Ablation Studies

Subsequently, we carry out ablation studies to evaluate the impact of individual refinement within DSAC-T.

1) *Learning stability*: As displayed in Fig. 3, DSAC-T outshines its variants, DSAC-T without critic gradient adjusting (which calculates the critic gradient using (13) instead of (18)) and DSAC-T with a single value distribution, in both learning stability and overall performance. This confirms the significant

TABLE II

AVERAGE FINAL RETURN. COMPUTED AS THE MEAN OF THE HIGHEST RETURN VALUES OBSERVED IN THE FINAL 10% OF ITERATION STEPS PER RUN, WITH AN EVALUATION INTERVAL OF 15,000 ITERATIONS. THE MAXIMUM VALUE FOR EACH TASK IS BOLDED.  $\pm$  CORRESPONDS TO STANDARD DEVIATION OVER 5 RUNS.

Task	DSAC-T	DSAC-v1	SAC	TD3	DDPG	TRPO	PPO
Humanoid-v3	<b>10937 <math>\pm</math> 345</b>	10092 $\pm$ 234	9335 $\pm$ 695	5631 $\pm$ 435	5291 $\pm$ 662	965 $\pm$ 555	6869 $\pm$ 1563
Ant-v3	<b>7076 <math>\pm</math> 202</b>	6324 $\pm$ 315	6427 $\pm$ 804	6184 $\pm$ 486	4549 $\pm$ 788	6203 $\pm$ 578	6156 $\pm$ 185
Halfcheetah-v3	<b>16641 <math>\pm</math> 724</b>	13580 $\pm$ 5637	16573 $\pm$ 224	8632 $\pm$ 4041	13970 $\pm$ 2083	4785 $\pm$ 967	5789 $\pm$ 2200
Inverteddoublependulum-v3	<b>9360 <math>\pm</math> 0</b>	9356 $\pm$ 1	<b>9360 <math>\pm</math> 0</b>	9347 $\pm$ 15	9183 $\pm$ 9	6259 $\pm$ 2065	9356 $\pm$ 2
Walker2d-v3	<b>6423 <math>\pm</math> 751</b>	6117 $\pm$ 530	6200 $\pm$ 263	5237 $\pm$ 335	4095 $\pm$ 68	5502 $\pm$ 593	4831 $\pm$ 637

TABLE III

AVERAGE RELATIVE VALUE ESTIMATION BIAS OVER 5 RUNS. THE RELATIVE BIAS IS COMPUTED USING  $\frac{\text{ESTIMATE Q-VALUE} - \text{TRUE Q-VALUE}}{\text{TRUE Q-VALUE}}$ , WHERE TRUE Q-VALUE IS ASSESSED BASED ON THE DISCOUNTED ACCUMULATION OF SAMPLED REWARDS. THE BEST VALUE IS BOLDED. WHEN BIASES ARE COMPARABLE, UNDERESTIMATION IS MORE FAVORABLE THAN OVERESTIMATION.

Task	DSAC-T	DSAC-v1	SAC	TD3	DDPG	TRPO	PPO
Humanoid-v3	<b>-5.15%</b>	24.21%	-11.12%	-38.57%	6.67%	3.33%	1.28%
Ant-v3	<b>-1.97%</b>	7.79%	-5.46%	-52.93%	22.95%	2.64%	1.56%
Halfcheetah-v3	0.86%	5.12%	<b>0.61%</b>	-38.19%	1.74%	-377.01%	22.20%
Inverteddoublependulum-v3	<b>0.14%</b>	1.15%	0.51%	-60.07%	6,288.32%	0.36%	0.21%
Walker2d-v3	<b>-0.76%</b>	7.91%	-0.97%	-11.44%	23.77%	0.39%	1.21%

contributions of the adjusted critic gradient, defined by (18), and the twin value distribution learning technique to learning stability and efficacy. Moreover, the ascending trajectory of the training curve reveals that the inclusion of the critic gradient adjusting refinement also accelerates learning by reducing gradient randomness.

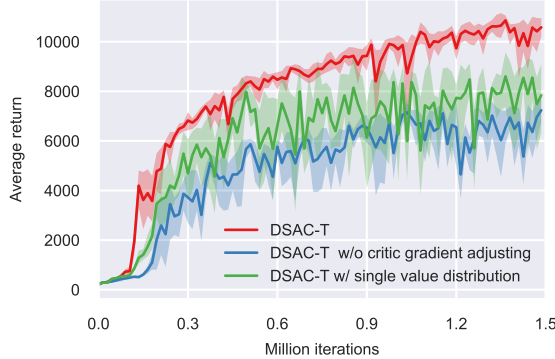


Fig. 3. Training curves in Humanoid-v3 over 5 runs, comparing ablation over critic gradient adjusting and twin value distribution learning.

2) *Sensitivity to reward scaling*: Fig. 4 illustrates the comparative performance of DSAC-T and DSAC-T with a fixed clipping boundary ( $b = 10$ ) across varied reward scales. DSAC-T maintains similar performance across diverse reward magnitudes, in contrast to DSAC-T ( $b = 10$ ), which exhibits significant sensitivity to the alterations in reward scales. This underscores the efficacy of implementing a variance-based clipping boundary, substantially diminishing the necessity for task-specific hyperparameter adjustments.

## VI. RELATED WORK

The concept of distributional RL, which involves modeling the distribution of returns with its expectation representing the value function, was initially introduced in [19]. Since then, numerous distributional RL algorithms have emerged, catering to both discrete control settings [20]–[24] and continuous

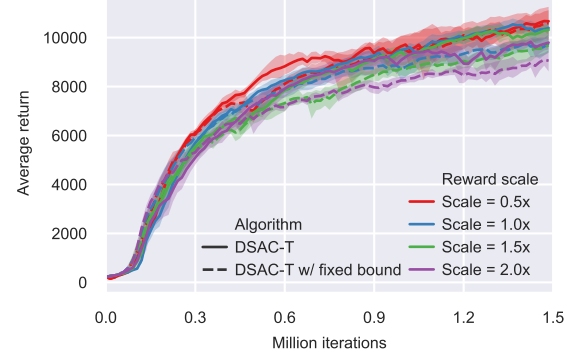


Fig. 4. Training curves in Humanoid-v3 over 5 runs with different reward scales, comparing ablation over variance-based target return clipping.

control settings [25], [26]. Building on the insights gained from distributional RL research, Dabney *et al.* [27] observed from mouse experiments that the brain represents potential future rewards not as a single mean but as a probability distribution.

Prevalent distributional RL studies typically shaped the value distribution utilizing either a discrete probability density function or a quantile function, resulting in a scenario where the mean value is not directly accessible but must be approximated based on a weighted average of finite quantiles. When the objective is to find a policy that maximizes the expected return, the evaluation accuracy of the mean value (i.e., Q-value) becomes crucial, even more so than the overall accuracy of the distribution. In this study, we directly learn a continuous probability density function for random returns, predicated on a Gaussian assumption, with Q-value as a direct output of the parameterized critic function. The theoretical findings presented in [11] demonstrate that this approach effectively mitigates Q-value overestimation. Furthermore, the introduction of twin value distribution learning has further reduced the overestimation bias, facilitating improved policy performance. Our ongoing work involves conducting a

comprehensive analysis of various value distribution learning methods to continue advancing the field of distributional RL.

## VII. CONCLUSION

In this study, we introduce an enhanced variant of the distributional soft actor-critic algorithm, termed DSAC with three refinements (DSAC-T), aimed at mitigating issues related to learning instability and sensitivity to reward scaling. These refinements encompass critic gradient adjusting, twin value distribution learning, and variance-based target return clipping. Specifically, we achieve improved stability by devising an adjusted critic update gradient, where the stable target Q-value replaces the random target return in the mean-related gradient. This is coupled with the deployment of a twin value distribution learning scheme. Empirical results substantiate the claim that these two refinements significantly improve the learning stability, thereby boosting the policy performance. To counter the reward scaling sensitivity, the third refinement introduces an adaptive variance-based boundary for clipping random target returns in the variance-related gradient. Experiment results demonstrate that DSAC-T exhibits a noteworthy performance enhancement when compared to mainstream model-free RL methods, including SAC, TD3, DDPG, PPO, and TRPO.

## REFERENCES

- [1] S. E. Li, *Reinforcement Learning for Sequential Decision and Optimal Control*. Springer Verlag, Singapore, 2023.
- [2] D. Silver, A. Huang, C. J. Maddison, A. Guez, L. Sifre, G. Van Den Driessche, J. Schrittwieser, I. Antonoglou, V. Panneershelvam, M. Lanctot, *et al.*, “Mastering the game of Go with deep neural networks and tree search,” *Nature*, vol. 529, no. 7587, p. 484, 2016.
- [3] D. Silver, J. Schrittwieser, K. Simonyan, I. Antonoglou, A. Huang, A. Guez, T. Hubert, L. Baker, M. Lai, A. Bolton, *et al.*, “Mastering the game of go without human knowledge,” *Nature*, vol. 550, no. 7676, p. 354, 2017.
- [4] V. Mnih, K. Kavukcuoglu, D. Silver, A. A. Rusu, J. Veness, M. G. Bellemare, A. Graves, M. Riedmiller, A. K. Fidjeland, G. Ostrovski, *et al.*, “Human-level control through deep reinforcement learning,” *Nature*, vol. 518, no. 7540, p. 529, 2015.
- [5] T. P. Lillicrap, J. J. Hunt, A. Pritzel, N. Heess, T. Erez, Y. Tassa, D. Silver, and D. Wierstra, “Continuous control with deep reinforcement learning,” in *4th International Conference on Learning Representations (ICLR 2016)*, (San Juan, Puerto Rico), 2016.
- [6] H. van Hasselt, “Double Q-learning,” in *23rd Advances in Neural Information Processing Systems (NeurIPS 2010)*, (Vancouver, British Columbia, Canada), pp. 2613–2621, 2010.
- [7] H. van Hasselt, A. Guez, and D. Silver, “Deep reinforcement learning with double Q-learning,” in *Proceedings of the 30th Conference on Artificial Intelligence (AAAI 2016)*, (Phoenix, Arizona, USA), pp. 2094–2100, 2016.
- [8] S. Fujimoto, H. van Hoof, and D. Meger, “Addressing function approximation error in actor-critic methods,” in *Proceedings of the 35th International Conference on Machine Learning (ICML 2018)*, (Stockholmsmässan, Stockholm Sweden), pp. 1587–1596, PMLR, 2018.
- [9] T. Haarnoja, A. Zhou, P. Abbeel, and S. Levine, “Soft actor-critic: Off-policy maximum entropy deep reinforcement learning with a stochastic actor,” in *Proceedings of the 35th International Conference on Machine Learning (ICML 2018)*, (Stockholmsmässan, Stockholm Sweden), pp. 1861–1870, PMLR, 2018.
- [10] T. Haarnoja, A. Zhou, K. Hartikainen, G. Tucker, S. Ha, J. Tan, V. Kumar, H. Zhu, A. Gupta, P. Abbeel, *et al.*, “Soft actor-critic algorithms and applications,” *arXiv preprint arXiv:1812.05905*, 2018.
- [11] J. Duan, Y. Guan, S. E. Li, Y. Ren, Q. Sun, and B. Cheng, “Distributional soft actor-critic: Off-policy reinforcement learning for addressing value estimation errors,” *IEEE transactions on neural networks and learning systems*, vol. 33, no. 11, pp. 6584–6598, 2021.
- [12] Y. Guan, S. E. Li, J. Duan, J. Li, Y. Ren, Q. Sun, and B. Cheng, “Direct and indirect reinforcement learning,” *International Journal of Intelligent Systems*, vol. 36, no. 8, pp. 4439–4467, 2021.
- [13] W. Wang, Y. Zhang, J. Gao, Y. Jiang, Y. Yang, Z. Zheng, W. Zou, J. Li, C. Zhang, W. Cao, *et al.*, “GOPS: A general optimal control problem solver for autonomous driving and industrial control applications,” *Communications in Transportation Research*, vol. 3, p. 100096, 2023.
- [14] T. Haarnoja, H. Tang, P. Abbeel, and S. Levine, “Reinforcement learning with deep energy-based policies,” in *Proceedings of the 34th International Conference on Machine Learning (ICML 2017)*, (Sydney, NSW, Australia), pp. 1352–1361, PMLR, 2017.
- [15] Y. Ren, J. Duan, S. E. Li, Y. Guan, and Q. Sun, “Improving generalization of reinforcement learning with minimax distributional soft actor-critic,” in *23rd IEEE International Conference on Intelligent Transportation Systems (IEEE ITSC 2020)*, (Rhodes, Greece), IEEE, 2020.
- [16] E. Todorov, T. Erez, and Y. Tassa, “Mujoco: A physics engine for model-based control,” in *2012 IEEE/RSJ International Conference on Intelligent Robots and Systems (IROS 2012)*, (Vilamoura, Algarve, Portugal), pp. 5026–5033, IEEE, 2012.
- [17] J. Schulman, S. Levine, P. Abbeel, M. I. Jordan, and P. Moritz, “Trust region policy optimization,” in *Proceedings of the 32nd International Conference on Machine Learning (ICML 2015)*, (Lille, France), pp. 1889–1897, 2015.
- [18] J. Schulman, F. Wolski, P. Dhariwal, A. Radford, and O. Klimov, “Proximal policy optimization algorithms,” *arXiv preprint arXiv:1707.06347*, 2017.
- [19] M. G. Bellemare, W. Dabney, and R. Munos, “A distributional perspective on reinforcement learning,” in *Proceedings of the 34th International Conference on Machine Learning (ICML 2017)*, (Sydney, NSW, Australia), pp. 449–458, PMLR, 2017.
- [20] W. Dabney, M. Rowland, M. G. Bellemare, and R. Munos, “Distributional reinforcement learning with quantile regression,” in *Proceedings of the 32nd Conference on Artificial Intelligence (AAAI 2018)*, (New Orleans, Louisiana, USA), pp. 2892–2901, 2018.
- [21] W. Dabney, G. Ostrovski, D. Silver, and R. Munos, “Implicit quantile networks for distributional reinforcement learning,” in *Proceedings of the 35th International Conference on Machine Learning (ICML 2018)*, (Stockholmsmässan, Stockholm Sweden), pp. 1096–1105, PMLR, 2018.
- [22] D. Yang, L. Zhao, Z. Lin, T. Qin, J. Bian, and T.-Y. Liu, “Fully parameterized quantile function for distributional reinforcement learning,” *Advances in neural information processing systems*, vol. 32, 2019.
- [23] M. Rowland, R. Dabashi, S. Kumar, R. Munos, M. G. Bellemare, and W. Dabney, “Statistics and samples in distributional reinforcement learning,” in *Proceedings of the 36th International Conference on Machine Learning (ICML 2019)*, (Long Beach, CA, USA), pp. 5528–5536, PMLR, 2019.
- [24] B. Mavrin, H. Yao, L. Kong, K. Wu, and Y. Yu, “Distributional reinforcement learning for efficient exploration,” in *Proceedings of the 36th International Conference on Machine Learning (ICML 2019)*, (Long Beach, CA, USA), pp. 4424–4434, PMLR, 2019.
- [25] G. Barth-Maron, M. W. Hoffman, D. Budden, W. Dabney, D. Horgan, D. TB, A. Muldal, N. Heess, and T. P. Lillicrap, “Distributed distributional deterministic policy gradients,” in *6th International Conference on Learning Representations (ICLR 2018)*, (Vancouver, BC, Canada), 2018.
- [26] C. Tessler, G. Tennenholz, and S. Mannor, “Distributional policy optimization: An alternative approach for continuous control,” *Advances in Neural Information Processing Systems*, vol. 32, 2019.
- [27] W. Dabney, Z. Kurth-Nelson, N. Uchida, C. K. Starkweather, D. Hassabis, R. Munos, and M. Botvinick, “A distributional code for value in dopamine-based reinforcement learning,” *Nature*, pp. 1–5, 2020.